JOURNAL OF SOLID STATE CHEMISTRY **26**, 223–234 (1978)

Composition-Dependent Microhardness and Its Relationship to Bonding in Sodium Tungsten Bronzes

I. J. McCOLM AND S. J. WILSON*

School of Materials Science and Technology, Bradford University, Bradford 7, United Kingdom

Received January 3, 1978; in revised form March 22, 1978

The technique of microhardness measurements using diamond indenters is outlined and assessed for its potential use in quantifying bonding changes and studying reactions in nonstoichiometric crystals. Results are presented for both Vickers and Knoop hardness values on {001} and {011} crystal planes of cubic sodium tungsten bronzes, Na_xWO_3, with x in the range 0.5 to 0.75. The Knoop data show that in only one direction, ⟨110⟩ on {001}, is the hardness sensitive to changes in composition. Hardness in the ⟨110⟩ directions and the degree of anisotropy increase as the sodium content of the bronze increases. All the crystal faces examined showed marked anisotropic behavior, with ⟨110⟩ being about 50% harder than ⟨100⟩ on {001} faces, while on {011} planes hardness increases in the sequence $\langle 100\rangle:\langle 21\bar{1}\rangle:\langle 11\bar{1}\rangle \approx \langle 01\bar{1}\rangle$. Hardness results from isomorphous and isoelectronic ReO_3 are considered with the Na_xWO_3 data to show the dominant role played by Na^+–WO_3 matrix interactions in determining the properties of these materials. The results are discussed in terms of current bonding theories for bronzes.

Introduction

For widely nonstoichiometric compounds which are characterized by directional covalent bonding and which also exhibit metallic properties such as the transition metal carbide systems TaC_x ($0.7 < x < 1.0$), TiC_x ($0.8 < x < 1.0$), and $Zr_{1-x}Ta_xC$, changes in composition are accompanied by a monotonic change in the filling of valence and conduction bands while the crystal structure is basically unchanged. For such compounds the observed microhardness, as obtained from randomly oriented Vickers diamond indents in polycrystalline samples, shows a marked dependence on composition, having a range of 1000 kg mm^{-2} or more (*1–3*). The hardness exhibits a maximum in the above examples for valence electron concentrations in the range 8.2 to 8.4, which has been equated with a minimum density of electron energy states in the calculated band system for a Fermi surface corresponding to such a valence electron concentration. Hence, in these materials, it appears that maximum hardness corresponds to a situation where the bonding orbitals are occupied while the antibonding orbitals remain empty.

Sodium tungsten bronzes Na_xWO_3 are, like the above examples, widely nonstoichiometric while maintaining a defective cubic perovskite structure and showing metallic properties throughout the range $0.4 < x < 1.0$. The metallic conduction properties of cubic M_xWO_3 phases have been consistently explained by models which involve the solution of M as a cation into the WO_3 matrix with the transfer of the valence electrons to a delocalized conduction band based on the W–O matrix

---

* Present address: Department of Mineralogy, University of Cambridge.

0022-4596/78/0263-0223$02.00/0

Printed in Great Britain

orbitals. Support for this approach comes from NMR (*4*, *5*), from conductivity (*6*, *7*), from Mössbauer spectra of ^{151}Eu in Eu_xWO_3 (*8*), from Hall effect measurements (*6*, *9*), and more recently from X-ray photoelectron spectra where filling of the conduction band with increasing x is explicitly demonstrated (*28*, *29*). All these experimental data to a greater or lesser extent show that the M atom is completely ionized. Interest has centered on the origin of the conduction band (*10–12*), and until very recently (*30*) features of the electronic structures of the bronzes have been inferred from variations in such properties as electronic conductivity.

In the cubic perovskite structure of M_xWO_3 Goodenough views σ-bond formation as being due to interaction of linear sp_σ anionic hybrid orbitals with octahedral d^2sp^3 hybrid orbitals of the tungsten ions. The tungsten cation t_{2g} orbitals mix with half the oxygen anion p_π orbitals while the other half remain nonbonding. This results in a bonding π band with essentially anionic character and an antibonding π^* band of predominantly cationic $5d$ (t_{2g}) character. The additional valence electrons introduced by the solution of M into the WO_3 matrix are donated to this π^* conduction band. In this general bonding scheme the role of the valence electrons donated by M is emphasized at the expense of the general chemical nature of the M atom and no account is taken of any interactions between M^{n+} cations and the WO_3 lattice. This in spite of the fact that short interatomic distances are involved and that the anionic orbitals which are p_π relative to tungsten cations are p_σ relative to M^{n+} cations. Thus, any tendency to resultant M^{n+}–O^{m-} bonding could perturb the π^* band by competing for the oxygen p_π orbitals. In the alkali metal bronzes the M cation is essentially basic, but any increase in the acidity or in the formal valence of the M cation will lead to increased competition for the p_π orbitals and thus a narrowing of the π^* conduction band and a consequent increased tendency to localization of electrons.

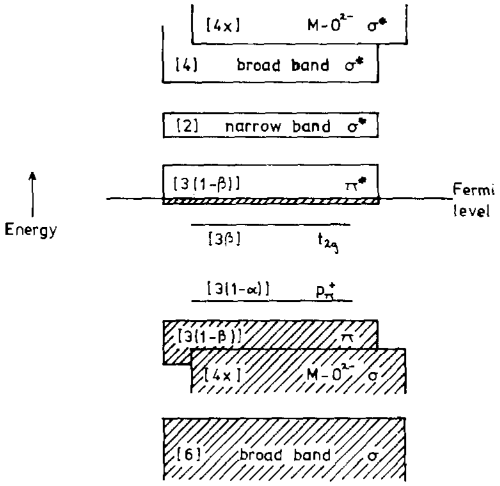

FIG. 1. Electronic energy band scheme for M_xWO_3 after Goodenough (*13*). Orbital degeneracies in brackets. $\alpha = 4x/3$ and $\beta = 0$ for $x \leqslant 0.75$ and $\alpha = 1, \beta = (4x/3) - 1$ for $x > 0.75$.

Goodenough (*13*) has presented a somewhat more refined model for Na_xWO_3, postulating interactions of Na^+ cations with the nonbonding p_π^+ oxygen orbitals in an attempt to explain the apparent anomaly in electrical conduction observed above $x = 0.75$ (*7*). This bonding scheme for sodium bronzes is shown in Fig. 1.

Recently Kopp *et al.* (*30*) have calculated the band structures for hypothetical cubic WO_3 and $NaWO_3$ from which their orbital densities of states show clearly the covalent nature of the bonding and provide further proof that a Na contribution to the conduction band in the density of states does not exist. However, the results do show that Na *d*, *p*, and *s* levels contribute throughout the valence band, thus substantiating the earlier hypothesis of Na^+–O interactions.

Since the change in electron concentration in band systems has been shown to have such large effects on the microhardness in cubic carbide systems it appeared feasible that the relative importance of band electrons and cation–matrix bonding might be elucidated in tungsten bronze systems from a study of composition–microhardness relationships.

Furthermore, it might be possible to monitor bronze reactions involving changes in numbers of electrons in bonding levels by this nondestructive potentially straightforward practical technique.

Concept of Hardness

Under the conditions existing in microhardness indentation testing most of the energy is expended on forming new surfaces whether by forcing up material round the indenter, by comminution, or by cracking the surface, so one is dealing in a direct sense with the strength of the chemical bonds in the material. However, the concept of hardness has no precise definition, as exemplified by its lack of recognized dimensions; some methods of measurement give it units of pressure while in others it is dimensionless. Even with the type of determination that involves indentation of a crystal surface the various hardness scales are not readily comparable.

In an indent test which involves the penetration of the surface of a crystal by a diamond indenter the measured hardness is a function of several parameters. This has led at various times to the concepts of tensile strength (*14*), ease of plastic flow (*1*, *15*), surface energy (*16*), and chemical bond strength (*1*, *2*, *17*) all being used in attempts to quantify measured hardness values. As examples of general factors which affect such a test the following are most notable.

First, grain size in polycrystalline samples has been shown to have an important effect when it is of the same order as the indent diameter (*18*). A decrease in grain size is accompanied by an increase in hardness as the dislocations generated by the indenter are blocked by the grain boundaries.

A second parameter requiring consideration is the applied load. If the load is too light and the indenter impression is shallow, then the microhardness will be dominated by the ease with which dislocations can glide in the near surface region. Thus, the nature of the surface will appear dominant. This has been shown to be important in the effect that adsorbed water has in reducing the microhardness of nonmetallic crystals such as SiC, MgO, and Al_2O_3 where a decrease in hardness occurs (*19*). This type of behavior is only observed, however, for small loads (less than 100g for MgO) and, thus, for small indent depths, and it may quite easily be masked by work hardening effects arising from polishing and surface preparation (*20*). Too great a load chosen for deep penetration to overcome these effects can result in brittle materials cracking and conchoidal fracture, which leads to measuring difficulties and erratic values as energy is expended in crack propagation. Hence, load selection is of some importance in determining the actucal magnitude of a measured hardness and the parameter sensitivity of the method. Selection must be done in a preliminary hardness against load study. From the formula for Vickers hardness, $H_V = (2 \cos 22°C\ P)/d^2$, the load P should be proportional to d^2, the square of the indent diagonal length. In practice a load should be chosen in a range where the relationship appears to hold best, for usually agreement is not $P = ad^2$ but $P = ad^n$, where n approaches 2, e.g., 1.9 for aluminium (*18*).

A third parameter associated with hardness value variations is temperature. There are several studies of the temperature dependence of microhardness in which Arrhenius type behavior allows calculation of activation energies characteristic of the thermally activated processes governing plastic flow in crystals (*1*, *15*, *21*). Thus, the role played by the crystal structure in determining microhardness values is a major one, since, apart from its effect on lattice energy, the actual arrangement of the atoms is important in determining the ease of plastic flow. In this respect too, the type of chemical bonding must be important since metallic or ionic bonding will prove less of a barrier to plastic flow than the strictly directed nature of covalent bonds. It should be noted that variations in microhardness observed as functions of indenter geometry and crystal orientation are in fact only reflections of different distributions of the shear stress within the bulk of the crystal.

Since there are so many factors which may be involved in determining microhardness, it is only when hardness variations follow composition changes within one crystal structure that chemical bonding theories are used to interpret the results (*2, 17, 22–24*).

The sodium tungsten bronzes, it was felt, represented a good system for the application of microhardness techniques to a chemical bonding study since relatively large crystals can be obtained, representing widely different compositions with essentially the same crystal structure, and a number of bonding models have been proposed. Hardness data from single crystals of Na_xWO_3 (x in the range 0.50 to 0.75), WO_3, and ReO_3 have been obtained for the first time and rationalized in terms of band filling effects and sodium ion–tungsten oxide lattice interactions.

Experimental Details

Single crystals of the cubic sodium bronzes were prepared by electrolytic reduction of molten mixtures of Na_2WO_4 and WO_3 (Koch-Light Ltd.) contained in either silica or alumina crucibles. Platinum electrodes with a 1-cm separation were used with a silica chimney around the anode to divert the liberated oxygen. Argon was flushed through the reduction cell during each experiment and the temperature was held just above the melting point of the charge while a constant voltage of 2 V was applied for 2 to 4 hr. Currents were in the range 10 to 50 mA. Electrodes with adhering crystals were freed from excess reactants by boiling briefly in dilute caustic soda solution. To obtain homogeneous crystals only short reduction times were used and all crystals were annealed *in vacuo* at 850°C from 5 to 17 hr.

Compositions were determined from the cubic lattice parameters obtained by Nelson–Riley extrapolation of Debye–Scherrer X-ray data and application of the Brown and Banks equation (*25*):

$$a_0 = 0.0819x + 3.7846\ \text{Å}.$$

Single crystals of ReO_3 were prepared by a method similar to that of Ferretti *et al.* (*26*) whereby powdered ReO_3 (Cerac Chemicals Ltd.) was sealed in an evacuated silica tube about 10 cm long with sufficient iodine to ensure the presence of the liquid throughout the experiment. The tube was heated in a temperature gradient from 40 to 390°C for 14 hr, during which time large ReO_3 crystals collected at the cool end. After washing with carbon tetrachloride the crystals were stored under fresh CCl_4 until required.

Crystals of WO_3 were prepared from Johnson and Matthey Ltd. spectroscopically pure reagent by vapor deposition in a closed platinum crucible in air at 1400°C.

For X-ray powder work a Philips 114.6-mm-diameter Debye–Scherrer camera using Ni-filtered copper $K\alpha$ radiation and a 57.3-mm-diameter Beaumauris Instruments Ltd. back-reflection Guinier camera, with tungsten as an internal standard, were used.

The back-reflection Laue method was used for identification and orientation of the single crystal faces. Unfiltered Mo radiation with a film-to-specimen distance of 5 cm was used. For $\{001\}$ cube faces it was necessary to use a 3-cm separation in order to increase the number of zones recorded for unambiguous identification.

For the sample containing only crystals with $\{011\}$ faces a (001) face was produced by grinding, checked by the Laue method, and then annealed under vacuum before being used to collect hardness data.

Hardness measurements were made on a Leitz "mini load" hardness apparatus using both Vickers and Knoop diamond indenters with loads in the range 50 to 500*g*. Specimens were mounted in Perspex and polished down to 1μm diamond paste but tests were also performed on unmounted, unpolished, annealed bronze crystals. Initially, random hardness tests were made but later a standard procedure was adopted. The Knoop diamond was aligned with its long axis along a desired crystallographic direction, or in the case of the Vickers indenter the diamond diagonals were aligned along convenient directions, before lowering slowly under a 200*g* load onto the crystal surface for 10 sec. In all cases from 4 to 30 determinations were made in order to obtain an average.

Indents, as well as being measured directly, were examined using a Nomarski interferometer to find the arrangement of ridges caused by the material displaced during the indenting process.

Results

For the sodium bronze crystals almost all the faces examined were within a few degrees of either the {001} or {011} planes after mounting and polishing. The largest deviation from perfect alignment was 8°, most of which is due to misalignment introduced by mounting, polishing, and Laue experimental error. However, if the deviation was as much as 8° the face was not used for hardness determinations. A marked variation of crystal habit with composition was observed between the higher and lower sodium content crystals. For $Na_{0.750}WO_3$ {001} faces were common while for $Na_{0.515}WO_3$ {011} faces occurred exclusively.

The ReO_3 crystals examined all had only {001} cubic faces well developed.

Vickers Microhardness Measurements

Mean values for 20 randomly oriented Vickers indents using a 100*g* load on at least three crystal faces for each composition are shown in Table I. First, it can be noted that compared to other widely nonstoichiometric systems the range of values is small. Second, there is a wide scatter in the results and therefore no relationship between hardness and

TABLE I

RANDOM VICKERS INDENTATION HARDNESS VALUES FOR SOME SODIUM BRONZE CRYSTALS

Composition Na_xWO_3 (x)	H_V (kg mm^{-2})
0.750	831 ± 200
0.601	841 ± 200
0.515	719 ± 180

TABLE II

ORIENTED VICKERS HARDNESS MEASUREMENTS

	Hardness (kg mm^{-2})[a]											
	{001} faces						{011} faces					
Composition:	$Na_{0.750}WO_3$		$Na_{0.601}WO_3$		$Na_{0.515}WO_3$		$Na_{0.750}WO_3$		$Na_{0.601}WO_3$		$Na_{0.515}WO_3$	
Load (*g*) / Diagonals along	$\langle 100 \rangle$	$\langle 110 \rangle$	$\langle 100 \rangle$	$\langle 110 \rangle$	$\langle 100 \rangle$	$\langle 110 \rangle$	$[100]$ and $[0\bar{1}1]$	$[1\bar{1}1]$ and $[2\bar{1}1]$	$[100]$ and $[0\bar{1}1]$	$[1\bar{1}1]$ and $[2\bar{1}1]$	$[100]$ and $[0\bar{1}1]$	$[1\bar{1}1]$ and $[2\bar{1}1]$
50	1100	799	1228	927	877	752	1069	936	954	734	850	859
100	974	724	1080	706	835	724	894	752	870	724	717	639
200	739	623	773	638		598	833	649	746	633	711	600
300	715	575		606		618	704	594	685	(610)[b]	623	560
500	585	538		(613)			656	557	(622)		(606)	

[a] Scatter in tabulated values is ±10%.

[b] Values within parentheses are less reliable because samples all cracked badly.

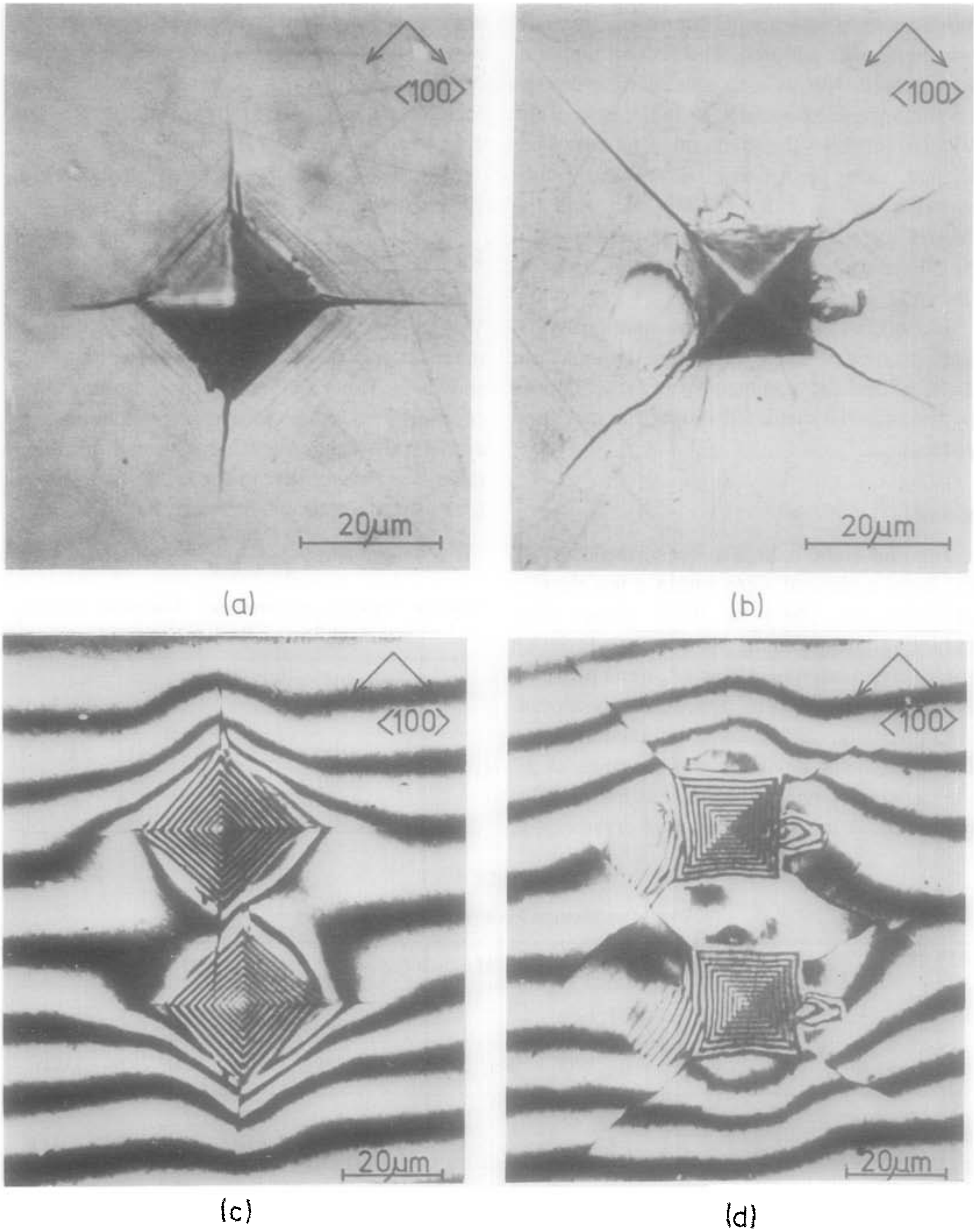

composition can be detected. Thus, more attention must be given to the details of the technique than for such systems as the cubic carbides.

Table II embodies several trends. First, there is the marked decrease in hardness with increasing load. Plots of log(load) against log(indent diagonal length) do not have slopes equal to 2, but lie in the range 1.57 to 1.75 for all the bronze crystals examined. This deviation from 2 may be the result of material piling up around the indent or of elastic

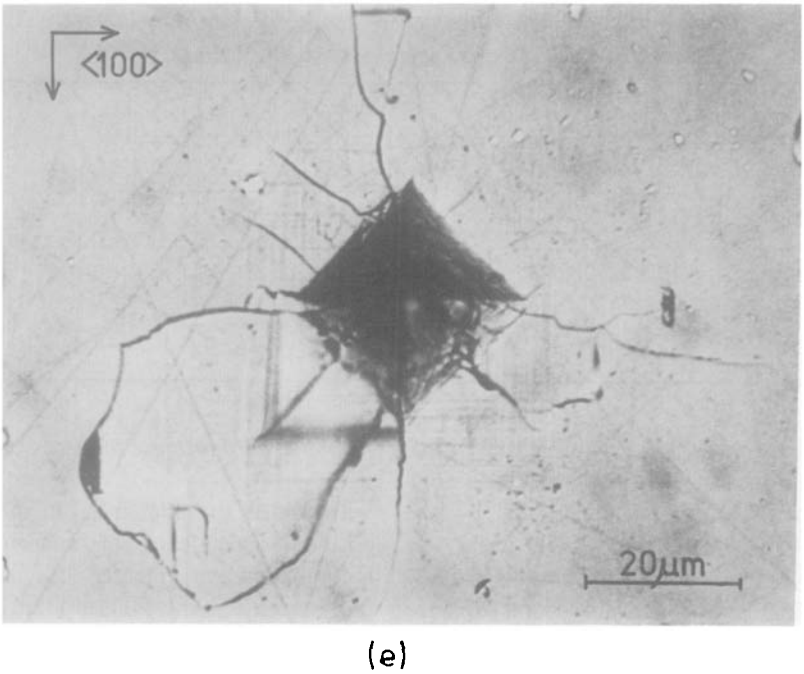

FIG. 2. Vickers indents on {001} faces of $Na_{0.75}WO_3$ crystals. (a, b) With 200g load. (c, d) 200g load, interference contrast. (e) 300g load.

recovery of the indents or of work hardening due to polishing. These factors may also have been responsible for the variations in the results.

For indents on {001} faces with diagonals along ⟨110⟩, displaced material is found near indent corners while for diagonals along ⟨100⟩ it appears along the indent sides. An example of this behavior is shown in Fig. 2, which also demonstrates the preferred cracking. Such variations in the position of displaced material obviously contribute to the hardness differences observed in different directions, since material at the corners will lead to a measured increase in *d*.

The correspondence between indent depth calculated from the number of interference fringes and those calculated from the diagonal length support the view that elastic recovery is not important. Agreement between the two depth calculations was within the overall 10% scatter in the data.

To test for work hardening effects the data were treated by plotting H_V against calculated indent depth. The results for the unpolished, annealed crystals produce the same shape of curve but such crystals were always softer than polished crystals. Thereafter a standard polishing procedure was adopted but, more important, a load ensuring penetration greater than 3 μm was always chosen.

The second major feature of the Vickers data in Table II is the role played by indenter orientation in determining hardness in these crystals. For {001} faces, hardness appears greater with indent diagonals aligned along ⟨100⟩ than along ⟨110⟩. For {011} faces it appears greater with alignment along [100] and $[01\bar{1}]$ than along $[1\bar{1}1]$ and $[2\bar{1}1]$. Dekker and Rieck (*22*) have noted that in a series of nonstoichiometric spinels the indenter orientation was a major factor in determining hardness on {001} faces. This they attributed solely to the piling up of displaced material around cracks that always formed along ⟨110⟩ irrespective of indenter orientation. Here we feel

TABLE III

KNOOP HARDNESS RESULTS FOR Na_xWO_3 CRYSTALS

Composition, x in Na_xWO_3	Hardness, H_K (kg mm^{-2})					
	{001}		{011}			
	⟨100⟩	⟨110⟩	⟨100⟩	⟨21$\bar{1}$⟩	⟨11$\bar{1}$⟩	⟨01$\bar{1}$⟩
0.515	475 ± 52	707 ± 57	445 ± 18	617 ± 25	685 ± 27	693 ± 28
0.601	500 ± 55	758 ± 68	391 ± 27	604 ± 42	671 ± 47	653 ± 46
0.691	502 ± 45	782 ± 63	—	—	—	—
0.750	497 ± 50	844 ± 34	—	—	—	—

that the data in Table II show a true anisotropy in hardness which is of greater importance than the explanation offered by the composition of displaced material. To probe this further the Knoop diamond indenter was used.

The third and most important feature arising from Table II is that there is a compositional dependence of hardness when the hardness of {011} faces is considered. As the sodium content increases, the hardness of the {011} face increases. This trend is not obvious for {001} faces.

Knoop Microhardness Measurements

In order to emphasize further the composition dependence of microhardness the Knoop diamond indenter was used. A constant load of 200g was used in all experiments. Mean values of measured hardnesses in important directions are shown in Table III and, in order to emphasize the anisotropy of hardness, orientation vs hardness curves are given in Fig. 3. Each data point is the average of from 3 to 18 indents on up to 4 crystals of

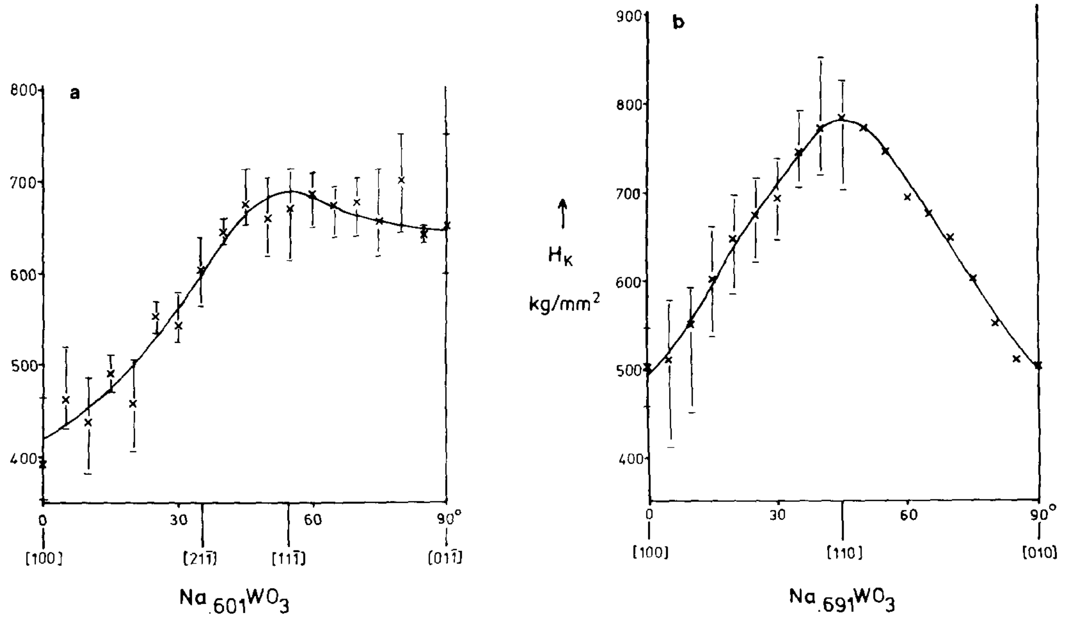

FIG. 3. Knoop hardness vs orientation plots for Na_xWO_3 single crystals: (a) {011} planes, (b) {001} planes.

the same composition. Average scatter in H_K lies around ±5% but does rise to 10% in samples which in certain orientations are susceptible to cracking.

For {001} faces, cracking and conchoidal fracture were observed to occur when the indenter was oriented along the hardest, ⟨110⟩, direction while for {011} faces cracking occurred when the long axis of the diamond was along the softer directions, i.e., within about 45° either side of [100] directions. Cracks in {011} faces often lay in $\langle 0\bar{1}1\rangle$ directions.

All the crystal faces examined showed marked anisotropy of hardness. For {001} faces, ⟨110⟩ directions were harder than ⟨100⟩ by about 50%, while for {011} faces the behavior was more complex with hardness increasing in the sequence $\langle 100\rangle:\langle 21\bar{1}\rangle:\langle 11\bar{1}\rangle \simeq \langle 01\bar{1}\rangle$.

The interesting conclusion to be drawn from the data for {001} faces in Table III is that the hardness of the ⟨110⟩ directions and the degree of anisotropy increases as the sodium content of the bronze increases. Thus, in order to study the composition dependence of micro-

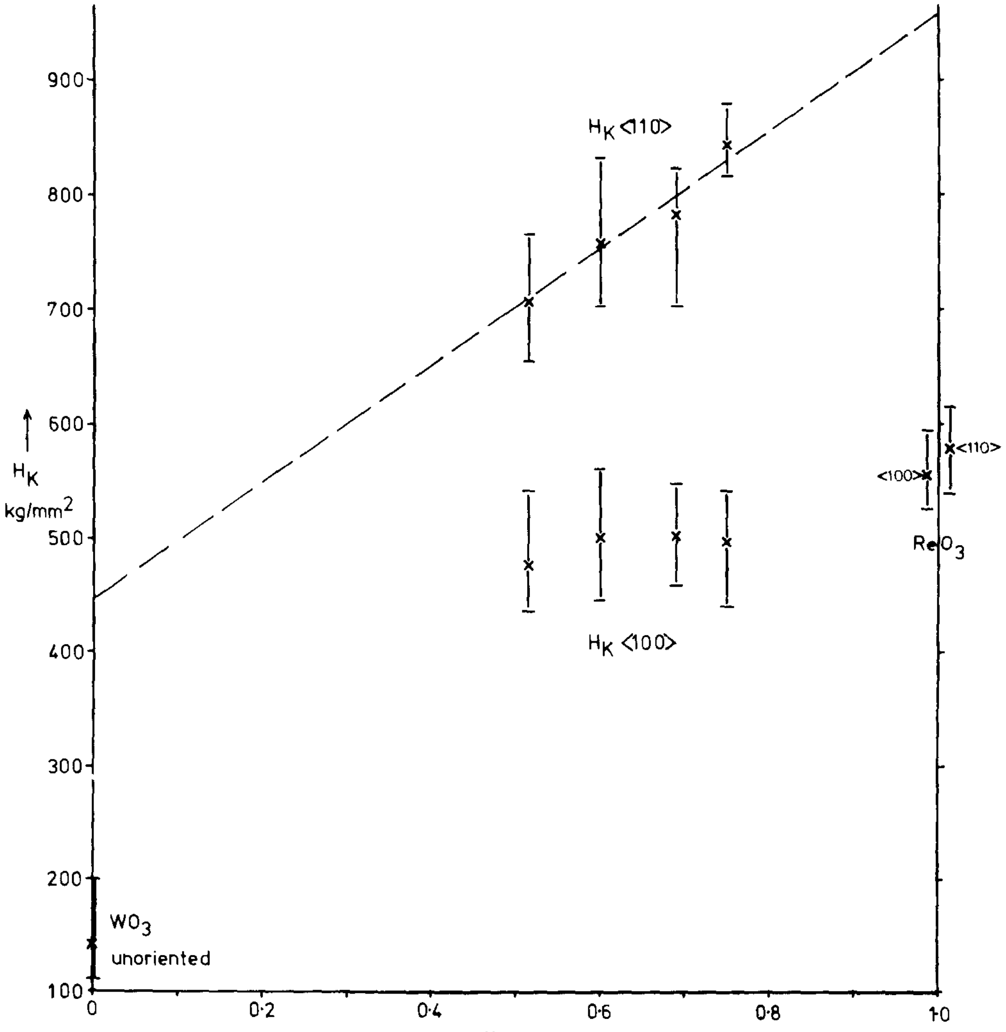

FIG. 4. Knoop hardness of {001} faces of Na_xWO_3 and ReO_3 crystals and of unoriented WO_3 crystals.

hardness in bronze systems, only Knoop data for ⟨110⟩ on {100} faces can be used. This point is emphasized in Fig. 4 where $H_{K\langle 110\rangle}$ and $H_{K\langle 100\rangle}$ are plotted against composition. Data for WO_3 and ReO_3 are also presented in Fig. 4. WO_3 has monoclinic symmetry and since only twinned crystals were obtained it was not possible to orient the samples. Hence, the data were obtained by making 36 indents at 10° increments on polished crystal faces to obtain the mean value of 142 ± 40 kg mm^{-2}.

The ReO_3 sample provided many suitable single crystals with {001} faces which enabled a series of 20 indents in ⟨100⟩ and ⟨110⟩ directions to be made. Unlike the sodium bronzes, only a small degree of anisotropy in hardness could be found:

$$H_{K\langle 100\rangle} = 555 \pm 30 \text{ kg mm}^{-2}$$

and

$$H_{K\langle 110\rangle} = 579 \pm 40 \text{ kg mm}^{-2}.$$

A curious feature of the indents in the ReO_3 crystals was that when immediately viewed it was not possible to measure them since no conditions of contrast would make them visible. After 10 to 15 min, however, the interior of the indent became yellow, which enabled the outline to be clearly seen against the red background of the crystal. Several hours after indentation the interior appeared to be pitted and full of interference colors but no change in indent outline length with time was observed after it first became visible. The yellow color may be diagnostic of events occurring beneath the indenter, for ReO_3 is known to disproportionate to ReO_2 and yellow Re_2O_7 at about 400°C (*26*). Thus, there may be here an indication of a considerable temperature rise. On the other hand, since the yellow color only appears slowly after indentation it more likely indicates enhanced room temperature oxidation at dislocations emerging at the surface. A very large dislocation density and its close confinement to the indent edges has been observed with the aid of electron microscopy in samples such as Nb_6C_5 (*27*).

Discussion

A major finding of this work is the care that has to be taken to reveal a composition dependence of microhardness and further that the dependence is only obvious when the anisotropic behavior of the system is investigated in a Knoop as opposed to a Vickers study of hardness.

The main aim of the work was to reveal the form of any hardness–composition relationship and compare any trends with those expected from current bonding theories. Therefore, the most important result arising from these experiments is that the hardness in ⟨110⟩ on {001} planes increases as the sodium content of the bronze increases, at least up to $x = 0.75$. This is in disagreement with the prediction based on the filling of an antibonding conduction band by electrons from the sodium atoms (*10–12, 30*) which, if this were dominant, would suggest that microhardness should decrease as the π^* band is populated. Furthermore, extrapolation of the hardness vs composition plot of Fig. 4 to predict the behavior expected from $Na_{1.0}WO_3$ and cubic WO_3 also suggests that the filling of the conduction band is not important. The hardness of cubic WO_3 cannot of course be tested, random indents on twinned monoclinic WO_3 crystals showing only that it is much softer than the sodium bronzes. ReO_3, on the other hand, by virtue of its small degree of anisotropy, appears to behave in a manner closer to that expected for cubic WO_3 than for the isoelectronic $NaWO_3$. The very close similarity between the electronic structure of Na_xWO_3 and ReO_3 has been visibly demonstrated in the X-ray photoelectron spectroscopic work of Campagna *et al.* (*29*). Thus, it appears that in perovskite bronze systems, the increase in hardness reflects the more important role played by the M–O^{2-} σ band in determining bronze properties, as postulated by Goodenough (*13*) and demonstrated by Kopp *et al.* (*30*). Figure 1 shows that if the decrease in electron energies due to cation–lattice interactions outweighs the effect of increased population of the π^* level, then an increase in x will lead to an overall increased bond strength. It can be seen that for $x < 0.75$ addition of a single sodium atom to the system results in one electron being added to the conduction band but also the transfer of eight electrons from the p_π^+ nonbonding level to the Na–O^{2-} σ band. In this manner, for x up to 0.75, an increase in bonding strength with Na concentration can be accounted for and so too the observed increase in hardness. The region with $x > 0.75$ is of interest in this context but so far it has not been possible to produce satisfactory single crystals with x above 0.75 free from sodium tungstate inclusions.

On the basis of the above model the hardness behavior of ReO_3 may be understood. Since the cation–lattice interactions appear to be more important than the concentration of conduction electrons in determining hardness, the fact that ReO_3, with its vacant perovskite M sites, shows behavior more like that expected for cubic WO_3 than for the isoelectronic $Na_{1.0}WO_3$ can be accounted for.

An alternative interpretation of the results might be in terms of the suggestion of Gilman (*17*) that hardness is determined by the size of the band gap for if Na^+–WO_3 interactions are lowering the energy of the bonding states then the band gap is increasing. Certainly the calculations of energy band positions by Kopp *et al.* (*30*) show that there are slight shifts of some of the valence bands toward lower energy and a slight rise of the conduction bands caused by their increased occupation when considering hypothetical cubic WO_3 and $Na_{1.0}WO_3$. Thus, when bonds are broken during the hardness test electrons are excited to the conduction band, or, at least, to nonbonding levels, and this becomes increasingly more difficult as x increases. The small effect noted by Kopp *et al.* may then correlate with the rather small change in hardness.

Both the above explanations for the increase in hardness rely on an important contribution to the lattice energy from Na–lattice interactions.

Further evidence for the importance of such interactions can be found in the thermochemical work of Dickens *et al.* (*31*, *32*), where attempts have been made to calculate values for the bonding energies of Na^+, H^+, and NH_4^+ bronzes. Differences in enthalpy changes for the system $M^+_{(g)} + (1/x)WO_{3(s)} + e^-_{(g)} \rightarrow (1/x)M_xWO_{3(s)}$ suggest that cation–lattice intractions are important.

In bronze systems then it seems that the cation–lattice interactions are very important in determining properties.

Acknowledgments

We express grateful thanks to the Royal Society for assistance by way of a grant to purchase the microhardness and X-ray equipment. The assistance of S.R.C. and Bradford University in providing a studentship for S.J.W. is also acknowledged.

References

1. G. M. Schwab and A. Krebs, *Planseeber. Pulvermetall.* **19**, 91 (1971).

2. S. P. Denker, *J. Less Common Metals* **14**, 1 (1968).

3. S. S. Ordanyan, L. V. Kudryasheva, and V. N. Fishchev, *Inorg. Mater.* **9**, 1529 (1973).

4. A. Narath and D. C. Wallace, *Phys. Rev.* **127**, 724 (1962).

5. D. P. Tunstall, *Phys. Rev. B* **11**, 2821 (1975).

6. L. D. Muhlestein and G. C. Danielson, *Phys. Rev.* **158**, 825 (1967).

7. W. R. Gardner and G. C. Danielson, *Phys. Rev.* **93**, 46 (1954).

8. C. S. Dimbylow, I. J. McColm, C. M. P. Barton, N. N. Greenwood, and G. E. Turner, *J. Solid State Chem.* **10**, 128 (1974).

9. E. J. Huibregtse, D. B. Barker, and G. C. Danielson, *Phys. Rev.* **84**, 142 (1951).

10. A. R. Mackintosh, *J. Chem. Phys.* **38**, 1991 (1963).

11. M. J. Sienko, "Nonstoichiometric Compounds," Advances in Chemistry Series, Vol. 39, p. 224, Amer. Chem. Soc., Washington, D.C. (1963).

12. J. B. Goodenough, "Progress in Solid State Chemistry" (H. Reiss, Ed.), Vol. 5, p. 145, Pergamon, New York (1971).

13. J. B. Goodenough, *Bull. Soc. Chim. Fr.* **41**, 1200 (1965).

14. D. M. MARSH, *Proc. Roy. Soc. (London) Ser. A.* **279**, 420 (1964).
15. D. L. KOHLSTEDT, *J. Mater. Sci.* **8**, 777 (1973).
16. M. V. SWAIN, R. M. LATANISION, AND A. R. C. WESTWOOD, *J. Amer. Ceram. Soc.* **58**, 372 (1975).
17. J. J. GILMAN, "The Science of Hardness Testing and Its Research Applications" (J. H. Westbrook and H. Conrad, Eds.), p. 51, Amer. Soc. Met. (1973).
18. H. BÜCKLE, "L'essai de Microdureté et ses applications," Publications Scientifiques et Techniques de l'Air, N.T. 90, Paris (1960).
19. A. R. C. WESTWOOD, N. H. MACMILLAN, AND R. S. KALYONCU, *J. Amer. Ceram. Soc.* **56**, 258 (1973).
20. A. MIYOSHI, A. HARA, AND Y. SUGIMOTO, *Planseeber. Pulvermetall.* **15**, 187 (1967).
21. M. S. KOVALCHENKO, V. V. DZHEMELINSKII, V. N. SKURATOVSKII, AND Y. G. TKACHENKO, *Inorg. Mater.* **9**, 1525 (1973).
22. E. H. L. J. DEKKER AND G. D. RIECK, *J. Mater. Sci.* **9**, 1839 (1974).
23. T. ITO AND T. YAMADA, *J. Amer. Ceram. Soc.* **58**, 80 (1975).
24. J. R. STEPHENS AND W. R. WITZKE, *J. Less Common Metals* **29**, 371 (1972).
25. B. W. BROWN AND E. BANKS, *J. Amer. Chem. Soc.* **76**, 963 (1954).
26. A. FERRETTI, D. B. ROGERS, AND J. B GOODENOUGH, *J. Phys. Chem. Solids* **26**, 2007 (1965).
27. G. MORGAN AND M. H. LEWIS, *J. Mater. Sci.* **9**, 349 (1974).
28. J. N. CHAZALVIEL, M. CAMPAGNA, G. K. WERTHAM, AND H. R. SHANKS, *Phys. Rev. B* **16**, 697 (1977).
29. M. CAMPAGNA, G. K. WERTHEIM, H. R. SHANKS, F. ZUMSTEG, AND E. BANKS, *Phys. Rev. Lett.* **34**, 738 (1975).
30. L. KOPP, B. N. HARMON, AND S. H. LIU, *Solid State Commun.* **22**, 677 (1977).
31. P. G. DICKENS AND D. J. NEILD, *J. Chem. Soc. Dalton* 1074 (1973).
32. P. G. DICKENS AND P. J. WISEMAN, *in* "MTP International Review of Science, Inorganic Chemistry Series, 2" (L. E. J. Roberts, Ed.), Vol. 10, Chap. 7, Butterworth, London (1975).